

Assessing Caval Flow Distribution in Patients with Fontan Circulation using 4D Flow MRI and Probabilistic Flow Connectivity Mapping

Kelly Jarvis^{1,2}, Susanne Schnell¹, Alex J Barker¹, James Carr¹, Joshua D Robinson^{3,4}, Cynthia K Rigsby^{1,4}, and Michael Markl^{1,2}

¹Radiology, Northwestern University, Chicago, IL, United States, ²Biomedical Engineering, Northwestern University, Chicago, IL, United States, ³Pediatrics, Northwestern University, Chicago, IL, United States, ⁴Medical Imaging and Cardiology, Ann & Robert H Lurie Children's Hospital of Chicago, IL, United States

Introduction: Hypoplastic left heart syndrome and other forms of single ventricle physiology are the most severe congenital heart diseases and typically require multiple successive surgical interventions to achieve palliation. The final surgical procedure creates the Fontan circulation which results in systemic venous return being supplied directly to the lungs through the pulmonary arteries without passing through the systemic ventricle.¹ Non-uniform caval flow distribution in Fontan circulation is suspected to cause pulmonary arteriovenous malformations, leading to negative outcomes.² 4D flow MRI can be employed for the comprehensive assessment of caval flow distribution to the left and right pulmonary arteries (LPA and RPA) by 3D flow visualization. Previous studies have used 4D flow MRI to quantify flow distribution by following traces of flow pathlines originating in the caval veins and reaching the LPA or RPA^{3,4} using a traditional 3D flow visualization method based on single pathlines (from one emitter point, a single pathline is calculated, Figure 1a). However, as with any velocity measurement, the acquired data includes noise uncertainties that can affect the magnitude and orientation of the measured flow velocity vector field. When visualizing flow pathlines, velocity measurement uncertainties may propagate over each time-step in the cardiac cycle and thus create uncertainties in the quantification of flow distribution. Recently, a new approach utilizing 3D probabilistic flow connectivity mapping has been presented for directly integrating local estimates of velocity noise into the analysis to report the level of statistical accuracy in 3D flow visualization⁵. This approach is based on the distribution of possible flow trajectories (from one emitter point, multiple possible pathlines are calculated, Figure 1b). It was the aim of this study to systematically analyze 3D probabilistic flow connectivity mapping and the influence of velocity noise on pathline visualization and thus uncertainty in the resulting flow distribution to the LPA and RPA in Fontan patients.

Methods: 4D flow MRI (FOV = 300-340 x 180-280 mm², slab thickness = 101-145 mm, resolution: spatial = 2.3-3.6 x 1.8-2.5 x 2.2-3.3 mm³, temporal = 38.4-41.6 ms, velocity sensitivity (venc) = 1-1.5 m/s, TR = 4.8-5.2 ms, TE = 2.4-2.7 ms, flip angle = 15°, band width = 450 MHz/pixel) was performed in a 1.5T system (Avanto, Aera, Siemens, Germany) in 7 patients (age = 15+/-6 [5-21] years, 2 females) with Fontan circulation (3 lateral tunnel, 4 extracardiac). A time-averaged 3D phase contrast angiogram was calculated using 4D flow MRI data to provide an enhanced depiction of cardiovascular geometry. 3D segmentation (Mimics Innovation Suite, Materialise, Belgium) was performed to create a 3D geometry of the Fontan connection to mask the velocity data. 3D probabilistic flow connectivity mapping was developed for in-vivo Fontan velocity datasets (Matlab, The MathWorks, USA). Random Gaussian noise distributions were generated with standard deviations = 0 (no noise), 0.02 m/s, 0.04 m/s, 0.06 m/s, 0.08 m/s and 0.10 m/s to reflect velocity noise ranging from 0-10% of a typical venc of 1 m/s. Noise was added independently to each voxel inside the segmented Fontan geometry for each velocity component (V_x, V_y, V_z). To improve pathline resolution, the noise-added velocity dataset was linearly interpolated in x, y, z and time with a refinement factor of 1. Pathlines were calculated from emitter points equally spaced in the inferior and superior vena cava (IVC and SVC) (Figure 2: left). The application of noise and pathline calculation was repeated 100 times in a Monte Carlo-type simulation approach. For each pathline calculation, flow distribution was quantified by the number of pathlines reaching the RPA or LPA normalized to the total number reaching either side. Probabilistic flow distribution at each noise level was quantified as the *mean +/- standard deviation (or uncertainty)* of the simulation results (Figure 2: right). In addition, for each patient dataset in this cohort, true velocity noise was estimated by calculating the standard deviation of velocities in areas of static tissue.

Results: Figure 3 shows the results for all 7 Fontan patients. The *mean* flow distribution remained consistent across noise levels, except for two datasets showing a drift greater than 5% (-13% for SVC flow in patient 1 and -14% for IVC flow in patient 5). The *standard deviation* of flow distribution measurements showed an increase for all datasets (ranging 0.3-10%) with levels of applied noise. At the true estimated noise level for each patient, uncertainty ranged 1-4% (Table 1) and in two datasets there was a drift in mean flow distribution greater than 0.5% from the no noise level (-2% for SVC flow and 1% for IVC flow for patient 1 and -1% for IVC flow for patient 7).

Conclusions: The findings of this study demonstrate that probabilistic flow connectivity mapping is useful for assessing the uncertainty of flow distribution quantification using 4D flow MRI in Fontan circulation. Low true velocity noise levels (at 0.03 m/s or below) show 4D flow is a robust method for flow distribution quantification. At these low noise levels, uncertainty (as defined by the standard deviation in simulations) remains small (1-4% in this study). However, two patient datasets showed mean flow distribution drift of +/- 1-2% not reflected in the uncertainty value. Further study is needed to best incorporate mean drift into the uncertainty value and to evaluate the clinical implications of flow distribution uncertainty levels.

Acknowledgment: Grant support by NIH R01HL115828, K25HL119608 and AHA 14PRE18620016.

References: 1. Gewillig. *Heart*, 2005;91:839-846. 2. Shah et al. *Ann Thorac Surg*. 1997;63:960-3. 3. Jarvis et al. *21st ISMRM*. 2013: abstract 812. 4. Bachler et al. *Radiology*. 2013;267:67-75 5. Friman et al. *Med Image Anal* 2011;15:720-728.

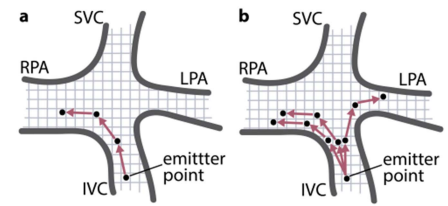


Figure 1: Theoretical drawings of 3D flow visualization based on (a) traditional single pathline method and (b) probabilistic method with three possible pathlines for the same emitter point.

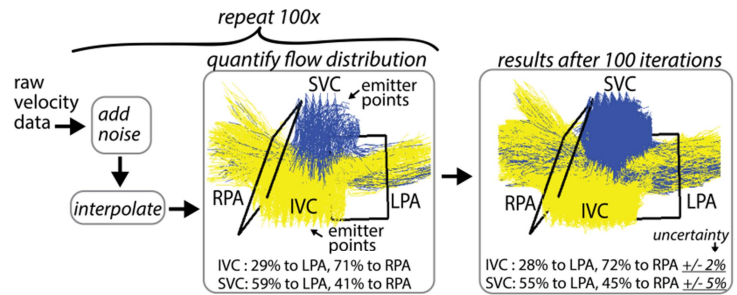


Figure 2: For each noise level, random noise was added to the velocity data and flow pathlines were calculated 100 times to quantify IVC flow (yellow) and SVC flow (blue) distribution to the LPA and RPA. Images are of patient 1 with noise level of 0.04 m/s.

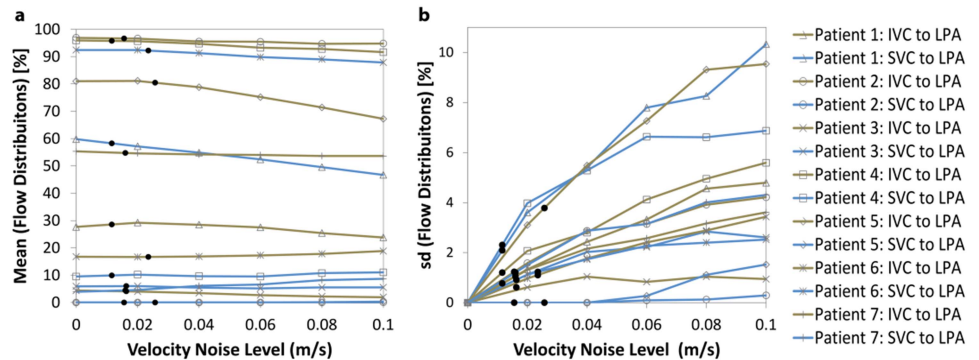


Figure 3: Probabilistic flow connectivity mapping results. The (a) mean and (b) standard deviation of flow distributions are shown for 100 iterations at each noise level. For simplicity, flow distribution results are only shown for the LPA because the results are normalized to the total number of pathlines reaching either side (flow distribution to RPA = 100% - flow distribution to LPA). True estimated noise values are noted by a black circle.

Patient	1	2	3	4	5	6	7
True velocity noise (m/s)	0.01	0.02	0.02	0.01	0.03	0.02	0.02
IVC flow to LPA (%)	29 +/- 1	97 +/- 1	4 +/- 1	96 +/- 1	80 +/- 4	17 +/- 1	55 +/- 1
SVC flow to LPA (%)	58 +/- 2	0 +/- 0	6 +/- 1	10 +/- 2	0 +/- 0	92 +/- 1*	4 +/- 1

Table 1: True estimated velocity noise is reported, along with the associated probabilistic flow distribution from Figure 3 (shown as black circles in the graphs). *SVC flow includes hemiazzygous vein flow into the Fontan connection.